

Molecular cloning and phylogenetic analysis of cereal type II metacaspase cDNA from wheat

E. PISZCZEK^{1*}, M. DUDKIEWICZ² and M. SOBCZAK³

Department of Biochemistry¹, Department of Experimental Design and Bioinformatics²
and Department of Botany³, Warsaw University of Life Sciences,
159 Nowoursynowska, PL-02776 Warsaw, Poland

Abstract

A new cereal type II metacaspase full-length cDNA from wheat (*Triticum aestivum* L.) leaves, *TaeMCAII*, was for the first time successfully amplified and sequenced. The full-length sequence of the *TaeMCAII* cDNA of 1 551 bp contains a 1 218 bp open reading frame. The deduced protein encoded by the *TaeMCAII* cDNA consists of 405 amino acids with a calculated molecular mass of 44 kDa and an isoelectric point of 5.29. In response to wounding or heat shock, a similar sequence of ultrastructural events including the tonoplast rupture, chromatin condensation, degradation of chloroplasts and disappearance of cytoplasm and organelles were observed using transmission electron microscopy. As the observed changes in *TaeMCAII* mRNA level did not occur to be statistically significant wounding-induced programmed cell death (PCD) seems to be metacaspase-independent pathway. Interestingly, in PCD caused by a heat-shock treatment, the level of *TaeMCAII* mRNA remained unaltered until 48 h after the stress what suggests that *TaeMCAII* participates in later stages of PCD triggered by heat-shock. Phylogenetic analysis enabled to classify *TaeMCAII* as a type II metacaspase. Finally, homology modelling of the putative three-dimensional structure of the *TaeMCAII* protein and a topology analysis of its probable active site were performed.

Additional key words: heat shock, programmed cell death, *Triticum aestivum*, wounding.

Introduction

Programmed cell death (PCD) is a genetically controlled process responsible for cell elimination during the ontogenesis of plants and in their responses to biotic and abiotic stresses. In majority of cases PCD in plants occurs to be an autophagic process, sequestrating and degrading cell constituents in vacuoles (Liu *et al.* 2005). The sequence of proteolytic cascade during the pathway of autophagy in plants is still unknown. However, the investigations carried out on plant cells undergoing PCD have shown an increase in the activities of proteases that cleave synthetic caspase substrates (Bonneau *et al.* 2008). The observed caspase activities in plant cells on their way to PCD were designated as 'caspase-like'. *In silico* investigations at the end of 20th century have brought the discovery of distant caspase relatives named

metacaspases (Uren *et al.* 2000). Metacaspases are divided into type I and type II based on their sequence and structure similarity. Type I metacaspases have an N-terminal prodomain similarly to initiator and inflammatory caspases. Type II metacaspases lack such a prodomain, but they contain a linker region between large and small subunits. Moreover, metacaspases, like caspases, have a conserved catalytic His/Cys dyad and harbour two distinguishable domains in their tertiary structure (Uren *et al.* 2000, Vercammen *et al.* 2004). Because of their similarity to caspases, it was expected for some time that they would exhibit caspase-like activities. Unexpectedly, studies with recombinant metacaspases of *Arabidopsis thaliana* and *Picea abies* showed that they were unable to cleave caspase

Received 19 February 2010, accepted 11 May 2010.

Abbreviations: CASP - caspase; EST - expressed sequence tags; FM - Fitch-Margoliash clustering; HR - hypersensitive response; JTT - Jones-Taylor-Thornton modelling; MSA - multisequence alignment; ORF - open reading frame; PCD - programmed cell death; PDB - Protein DataBank; RACE - rapid amplification of cDNA ends; *TaeMCAII* - *Triticum aestivum* type II metacaspase; TEM - transmission electron microscopy.

Acknowledgements: This study was supported by a grant from Polish Ministry of Science and Higher Education No. N303 048837.

* Corresponding author; fax: (+48) 22 5932562, e-mail: ewa_piszczek@sggw.pl

substrates, but their preferred cleavage site was after the Arg or Lys residues (Vercammen *et al.* 2004 and 2006, Bozhkov *et al.* 2005). Thus, these results suggest that metacaspases are not responsible for the plant caspase-like enzyme activity. It is also expected that they should play a significant role in proteolytic events during PCD in plants (Watanabe and Lam 2004). Until now, there was no direct evidence to support this expectation. Results published so far seem to be rather conflicting but suggestive that some metacaspases may play a role in PCD and some may not (Hoeberichts *et al.* 2003, Baarlen *et al.* 2007, Castillo-Olamendi *et al.* 2007, Hao *et al.* 2007, He *et al.* 2008). Many investigations on the metacaspase role in PCD have been focused on their involvement in the hypersensitive response (HR) (Hoeberichts *et al.* 2003, Baarlen *et al.* 2007, Castillo-Olamendi *et al.* 2007, Hao *et al.* 2007). The infection of tomato leaves with *Botrytis cinerea* leads to an increased level of the type II metacaspase transcript, *LeMCA1*, suggesting its involvement in HR-related PCD (Hoeberichts *et al.* 2003). Interestingly, the *Nicotiana benthamiana* metacaspase gene, *NbMCA1*, did not appear to be involved in the PCD of non-host HR resistance to

Pseudomonas syringae, but it did decrease the susceptibility of *N. benthamiana* to *Colletotrichum destructivum*, indicating its function in a defence response (Hao *et al.* 2007). Other studies with leaves of *A. thaliana* infected with *Botrytis* sp. revealed that only type II metacaspases played a role in cell death during plant-pathogen interactions because mutants with knocked-out metacaspase genes were less susceptible to those pathogens. Conversely, mutations in the type I metacaspase genes caused *Arabidopsis* plants to be more susceptible to *Botrytis* species. The observed accelerated senescence of type I metacaspase mutants suggests that these proteases participate in the suppression of cell death (Baarlen *et al.* 2007).

This work provides the description of a newly identified type II metacaspase cDNA, *TaeMCAII*, from wheat leaves. Moreover, the involvement of *TaeMCAII* in PCD caused by wounding or heat shock was investigated by evaluating its transcript level. To get more information about its predictable role in wheat and to assess its relationship with other metacaspases, phylogenetic and bioinformatic analyses were performed.

Materials and methods

Plants and growth conditions: Spring wheat (*Triticum aestivum* L.) seedlings were grown in Hoagland nutrient solution for two weeks under controlled conditions (temperature of 20 °C, 16-h photoperiod, irradiance of 260 $\mu\text{mol m}^{-2} \text{s}^{-1}$ and relative humidity of 70 - 80 %). The plants were subjected to abiotic stresses (wounding or heat shock). For the wounding, the leaves of seedlings were punched with a razor blade. For the heat-shock treatment, seedlings were exposed to 50 °C for 20 min. Samples were collected 3, 8, 24 and 48 h after stress and were immediately processed for the ultrastructural analysis or frozen in liquid nitrogen and stored at -80 °C for the evaluation of the *TaeMCAII* transcript levels.

Cloning and sequencing of the *T. aestivum* type II metacaspase: The total RNA was isolated from wounded leaves according to the Chomczyński and Sacchi (1987) method. The total cDNA was obtained using the *Reverse Transcriptase System* (Promega, Madison, USA). Using the *Oryza sativa* sequence of the type II metacaspase gene (XP_475477), the GenBank database was searched for *T. aestivum* ESTs of type II metacaspases. A predicted sequence was created by merging several overlapping *T. aestivum* EST sequences. *T. aestivum* type II metacaspase fragment of 791 bp was amplified on cDNA template in PCR reactions with specific forward (5'-GTTGACCGCATGCACAAGTG-3') and reverse (5'-CCTTCAGGAAGTGGTGAGCTAG-3') primers. The PCR conditions were as follows: 2 min denaturation at 95 °C, 30 cycles of 1 min at 95 °C, annealing of the

primers for 30 s at 59 °C, extension for 45 s at 72 °C and a final extension for 5 min at 72 °C. The product of PCR was subcloned in the *pGEM-T-Easy* vector and sequenced.

5' and 3' rapid amplification of cDNA ends (RACE): The *GeneRacer*™ cDNA amplification kit (Invitrogen, Carlsbad, USA) and total RNA isolated from wounded plants were used to amplify the 5' and 3' ends of the *TaeMCAII* cDNA. Total RNA for 5' end amplification was prepared by dephosphorylation and removal of the cap. The *TaeMCAII* cDNA synthesis was performed with the *SuperScript*™ III reverse transcriptase and *Platinum® Tag* DNA high fidelity polymerase (Invitrogen). The ends of the *TaeMCAII* cDNA were amplified with the *Gene Racer* 3' and 5' primers supplied with the kit. For 3' and 5' ends amplification of the cDNA forward (5'-CTGTGATGAGCTGTGCACG AGAGGTTTC-3') and reverse (5'-ACTCGTCGTACCC GGTGTCGTCGTC-3') gene-specific primers were designed to the sequence, respectively. Touchdown PCR with these primers was performed under the following conditions: 2 min at 94 °C, 5 cycles of 30 s at 94 °C and 40 s at 72 °C; 5 cycles of 30 s at 94 °C and 40 s at 70 °C; 25 cycles of 30 s at 94 °C, 30 s at 65 °C and 40 s at 68 °C and 10 min of final extension at 68 °C. To establish the 3' cDNA end of *TaeMCAII* the obtained PCR product was used as a template in the nested PCR amplification reaction with the *GeneRacer*™ nested primer supplied with the kit and the forward nested gene-specific primer

(5'-GCCTACAAACGGCATCCTCATCAG-3') designed to the sequence of TaeMCA II. The thermal cycling conditions were as follows: 2 min at 94 °C, 35 cycles of 30 s at 94 °C, the annealing of the primer for 30 s at 62 °C and extension for 2 min at 68 °C and a final extension for 10 min at 68 °C.

All PCR reactions were performed using the 2720 thermal cycler (*Applied BioSystems*, Carlsbad, USA). The GenBank accession number for the established sequence of *TaeMCAII* is GU130248.

Ultrastructural analysis: Fragments of leaf blades (about 2 × 2 mm in size) were dissected with a razor blade and immediately immersed in a fixative composed of 2 % (m/v) paraformaldehyde and 2 % (v/v) glutaraldehyde in 0.1 M cacodylic buffer (pH 6.8). The samples were fixed at room temperature under a -0.04 MPa vacuum for 2 h. They were washed in the same buffer, dehydrated and embedded in *Epoxy Resin* (*Fluka*, Buchs, Switzerland) according to the procedure described by Golinowski *et al.* (1996) and Sobczak *et al.* (1997). Ultra-thin sections were made on a *Leica UCT* (*Leica Microsystems*, Nussloch, Germany) ultramicrotome. They were collected on single slot copper grids coated with *Formvar* film (*Fluka*) and stained with uranyl acetate and lead citrate (Golinowski *et al.* 1996, Sobczak *et al.* 1997). The sections were examined under an *FEI M268D Morgagni* (*FEI*, Hillsboro, USA) transmission electron microscope equipped with an *SIS Morada* (Münster, Germany) digital camera.

Relative quantitative RT-PCR: Total RNA isolated from *T. aestivum* leaves subjected to heat shock or wounding was treated with RNase-free DNase (*Sigma*, St Louis, MI, USA) according to the manufacturer's instructions. The prepared RNAs were used as templates in one-step RT-PCR reactions performed with gene-specific primers and titanium one-step RT-PCR kit (*Clontech Laboratories*, Mountain View, USA). Type II metacaspase-specific forward (5'-GTTGACCGCATGCA CAAGTG-3') and reverse (5'-CTGCTTGGTGCTATT GCCTATCTG-3') primers were designed to amplify the 399 bp RT-PCR product. As a control, the *T. aestivum* housekeeping gene *18SrRNA* was used. The forward (5'-GTGACGTCAAAGTACCAAGTG-3') and reverse (5'-CTAGCGATTCAACTTCATGTTC-3') primers were used to amplify its 365 bp fragment. The PCR conditions were as follows: 60 min at 50 °C, 5 min at 94 °C, 27 or 12 (for *18SrRNA*) cycles of 30 s at 94 °C, 30 s at 60 °C, 1 min at 68 °C and a final extension for 2 min at 68 °C. The PCR products were analysed by electrophoresis on a 1.2 % agarose gel stained with ethidium bromide. The excised and eluted fragments of *TaeMCAII* and *18SrRNA* genes were cloned into the *pGEM-T Easy* vector and sequenced. The band intensities

of the metacaspase and *18S rRNA* PCR products were measured by the *ImageJ* programme and compared for each gel lane. The relative expression was calculated by taking a ratio of the intensity of the metacaspase band over the intensity of the *18SrRNA* band. For statistical analysis of data the *ANOVA* test was used.

Bioinformatics analysis: Multisequence alignments (MSA) of the amino acid sequences of known plant metacaspases, homologs of *TaeMCAII*, were made using *Clustal X 1.83*. An *MSA* manual editing and analysis was performed with the help of the *GeneDoc 2.6.02* and *Jalview 2.3 MSA* analysis tools. The identification of the coding region, open reading frame and the translation of *TaeMCAII* nucleotide sequence were made based on the *FGENESH* gene structure prediction using an *HMM* model constructed for monocot plants (*SoftBerry* software <http://linux1.softberry.com/berry.phtml>). To ascertain the relationship among the plant metacaspases, two phylogenetic analyses were carried out: Fitch-Margoliash (FM) clustering based on the distance matrix calculations of the Jones-Taylor-Thornton (JTT) amino acid substitution matrix; a maximum likelihood (ML) clustering analysis based on the same JTT model (with a constant rate of change and one category of substitution rates). Analyses were performed using the algorithms from the *PHYLIP 3.69* programme package, *Phylogeny.fr* server (<http://www.phylogeny.fr>) and *ITOL* (Interactive Tree of Life - <http://itol.embl.de/index.shtml>) (Letunic and Bork 2007).

The bacterial putative caspase (peptidase C14) sequence of GSU0716 from *Geobacter sulfurreducens* and the crystal structure of this protein (PDB 3BIJ) were used as a root for phylogenetic tree and as a template for the homology modelling of *TaeMCAII* three-dimensional structure, respectively.

The template structure for the preliminary model of the *T. aestivum* type II metacaspase was selected based on the *FFAS03* server scores (*Fold & Function Assignment System* - an interface for a profile-profile alignment and fold recognition algorithm) (Rychlewski *et al.* 2000). They were also based on a comparison of the secondary structure prediction results for the *TaeMCAII* sequence and the secondary structure annotation for candidate structures resolved experimentally.

The proposed preliminary model of the *TaeMCAII* large subunit was made with the *Prime 4.5 Schrödinger®* fully integrated package for homology-based protein structure prediction. The generated alignment was manually edited. The loops in the neighbourhood of the putative substrate coordination pocket were refined after model building (Jacobson *et al.* 2004, Zhu *et al.* 2007). Obtained model has been validated using *MetaMQAP*, a metaserver for quality assessment of protein structures optimized for theoretical models (Pawlowski *et al.* 2008).

Results

Based on the combination of five *T. aestivum* expressed sequence tags (ESTs), TC344742, TC282514, TC292224, TC340820 and TC331470, a 791 bp fragment of the putative type II metacaspase was amplified. Subsequently, it was extended in both the 3' and 5' directions by the RACE PCR method and finally, a full-length cDNA of 1551 bp for the type II metacaspase from wheat was successfully estimated. The sequence of the full-length of *TaeMCAII* cDNA contains a 1218 bp open reading frame (ORF), a 199 bp + 25 polyA 3' untranslated region (3' UTR) and a 109 bp 5' UTR. *TaeMCAII* encodes a protein of 405 amino acids with a calculated molecular mass of 44 kDa and an isoelectric point of 5.29.

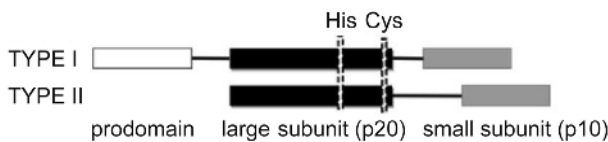


Fig. 1. Schematic presentation of metacaspase domains. The catalytic domains consist of large (p20) and small (p10) subunits. Positions of the catalytic Cys and His residues are indicated.

A *BLAST* analysis of the amino acid sequence of *TaeMCAII* revealed the presence of two conserved domains homologous to caspase-like sequences. At the N- and C-terminal sides of the predicted protein of *TaeMCAII*, the conserved regions corresponding to the large and small subunits of caspases can be distinguished, respectively. Between these two subunits, there is a linker region of about 100 amino acids (Fig. 1). The alignment of the amino acid sequences of the large subunits from both types of plant metacaspases (Fig. 2) showed that in all of the catalytic centres of the studied proteins, including the *TaeMCAII* putative protein, the characteristic amino acid triad, His 87, Gly 88 and Cys 140 (the numbering according to *T. aestivum* sequence), was conserved.

Based on the MSA analysis conducted on seven type II plant metacaspases, AtMC4, AtMC6, AtMC8, AtMC9, mcII-Pa, PsMCII and the newly identified *TaeMCAII*, the conserved amino acid residues involved in the substrate P1 coordination were distinguished to be Asp 26 and Asp 138 (in the large subunit) and Ser 336 in the small subunit. These residues aligned with the coordinating Asp present in the other analysed sequences at the same position of the MSA (Fig. 2).

Transmission electron microscopy (TEM) revealed that leaf blade cells subjected to heat stress displayed ultrastructural features typical for PCD. The most pronounced reaction occurred in the phloem bundle cells that were degenerated in all of the examined samples at 3 h after the stress cessation (Fig. 3a). In mesophyll cells,

progress of PCD was slower. Interestingly, different stages of PCD were often observed in neighbouring cells (Fig. 3b), where the cell on the left still has a continuous tonoplast, in the bottom cell there are ruptures in the tonoplast, and in the cell on the right the tonoplast is broken and retracted. Similar situations were observed also at other time points (data not shown). In samples collected 3 h after the heat treatment, most of the mesophyll cells had normal appearance (Fig. 3b,c). Mesophyll cells still had well-preserved protoplasts and central vacuoles, but in some cells tonoplast ruptures were present (Fig. 3b). Nuclei were round with slightly convoluted nuclear envelopes (Fig. 3c) and contained similar amounts of heterochromatin as in the non-stressed mesophyll cells. The most pronounced changes were observed in chloroplasts, which were usually round in sections, and their internal thylakoid system often lost its parallel arrangement (Fig. 3b). In some chloroplasts, the thylakoids were dispersed and swollen (Fig. 3c). In contrast to chloroplasts, the mitochondria were unchanged structurally in all examined samples. At the some parts of the cell walls, electron-translucent material similar to callose was deposited (Fig. 3b). In samples collected at 8 h after stress, most of the cells contained ruptures in the tonoplast. The number of chloroplasts with distorted and swollen thylakoids increased as well as the amount of heterochromatin (Fig. 3d). In samples collected 24 h after stress, most cells contained clumped protoplast accumulated at some places inside the cell lumen while the rest of the lumen was empty or contained only membranous debris (Fig. 3f). Nuclei became round in sections and contained strongly osmophilic heterochromatin (Fig. 3e). Chloroplasts had an abnormal ultrastructure (Fig. 3e,g), and some of them had lost their envelopes, leaving only remnants of the thylakoids (Fig. 3f). Depositions of electron-translucent material at the cell wall were numerous, especially at the regions containing plasmodesmata (Fig. 3f). They sometimes also enclosed membranous structures (Fig. 3g). 48 h after stress, many cells contained only the hardly recognisable debris of the cytoplasm and organelles (Fig. 3h). The cell walls were often ruptured thus allowing the leakage of protoplast debris into the intercellular spaces.

In the case of wound-stressed leaf blades, phloem cells in vascular bundles next to the wound were degenerated, similar to the situation observed in heat-stressed plants. However, vascular bundles more remote from the wound usually did not contain degenerated phloem cells. The ultrastructural changes occurring in mesophyll cells next to wound were, in general, similar to the above-described response to heat shock. They included changes in chloroplast ultrastructure, chromatin condensation, rupture of tonoplast and deposition of electron-translucent material at some parts of the cell walls. Similar to the mesophyll cells response to heat

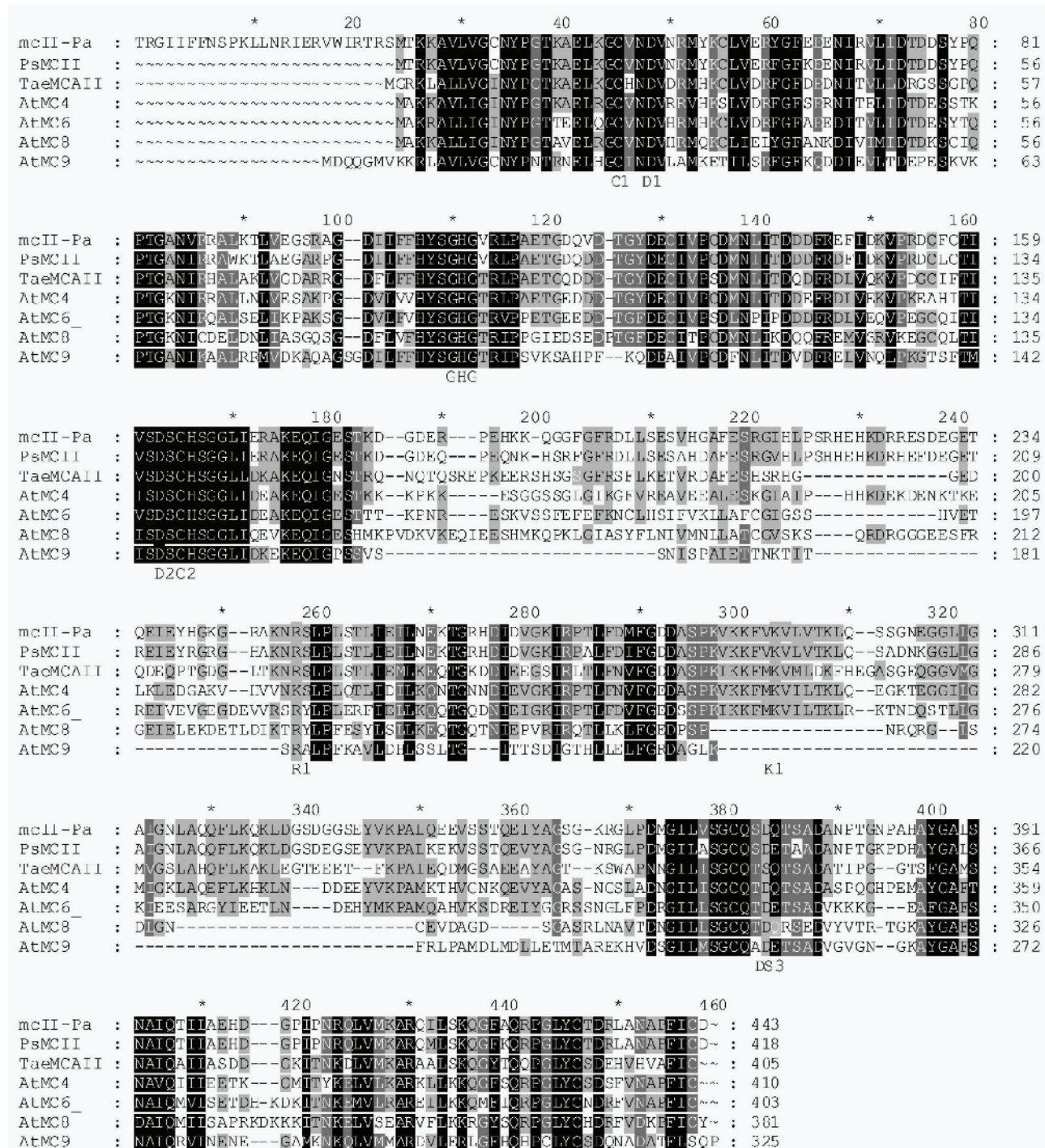


Fig. 2. MSA of known sequences of plant type II metacaspases. *Arabidopsis thaliana*: AtMC4 (NP_178052.1), AtMC6 (NP_178050.1), AtMC8 (NP_173092.1) and AtMC9 (NP_196040.1); *Pinus silvestris* (ACB11499.1) and *Picea abies* (CAD59226.1) and the newly obtained *T. aestivum* TaeMCAII sequence (ACY82389.1). Following domains and features are labelled and indicated: C1 - catalytic cysteine Cys 23 (Belenghi *et al.* 2007); D1 - conserved aspartate residue Asp 26 possibly involved in substrate P1 coordination (Vercammen *et al.* 2007); GHG - active site His 87 and Gly 88; D2 - Asp 138-residues building the pocket S: conserved aspartate residues involved in substrate P1 coordination; C2 - active site Cys 140; R1 - autocatalytic site (Arg 214 according to Vercammen *et al.* 2007); K1 - Lys 260-counterpart of *P. abies* Lys 269 supposed cleaving site (Bozhkov *et al.* 2005); DS3 - conserved residues possibly involved in substrate P1 coordination (in TaeMCAII sequence Ser 336, in residues in the rest of aligned sequences -Asp). Shading by conservation.

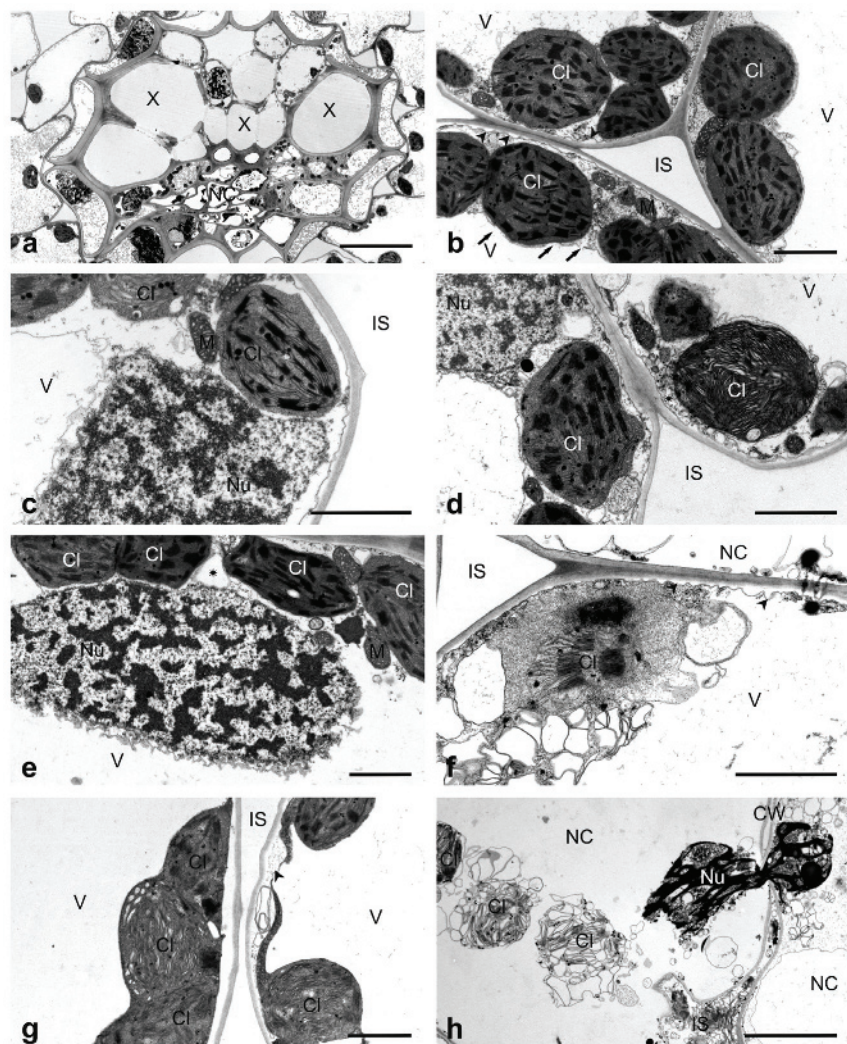


Fig. 3. The ultrastructural changes in wheat leaf blade cells during PCD induced by a heat-shock treatment. *a* - Cross section of a degenerated leaf bundle. *b* to *h* - Cross sections of mesophyll cells. *a* to *c* were taken from samples collected at 3 h post stress, *d* at 8 h, *e* to *g* at 24 h and *h* at 48 h. Abbreviations: Cl - chloroplast, CW - cell wall, IS - intercellular space, M - mitochondrion, NC - necrotised phloem bundle cells, Nu - nucleus, X - xylem, V - vacuole. Arrows indicate tonoplast breakages (*b*), arrowheads indicate the depositions of electron-translucent material at the cell wall (*b*, *f* and *g*). Bars: *a* - 10 μ m; *b* to *g* - 2 μ m; *h* - 5 μ m.

Table 1. The expression of *TaeMCAII* gene in wheat leaves subjected to wounding and heat-shock treatment. The amount of *TaeMCAII* mRNA was determined relative to the amount of *18S rRNA*. The mean relative expression values are shown with standard deviation calculated from three replicates. * - value significantly different at $P < 0.05$ from wheat leaves 0 h post heat-shock treatment according to one way ANOVA.

Time after stress [h]	0	3	8	24	48
Wounding	1.46 ± 0.79	1.90 ± 0.14	1.20 ± 0.00	2.13 ± 0.24	1.68 ± 0.67
Heat-shock	0.65 ± 0.07	0.81 ± 0.07	0.80 ± 0.07	0.81 ± 0.13	$1.05 \pm 0.06^*$

shock, their response to wounding was not temporally coordinated, and different stages of PCD occurred in neighbouring cells. In opposition to PCD induced by heat shock, no cell-wall breakages and leakage of protoplast remnants into the intercellular spaces was observed.

The transcript levels of the *TaeMCAII* gene were evaluated in wheat leaves following the wounding or heat shock that lead to PCD, as revealed by the TEM analysis. The accumulation of the *TaeMCAII* transcript was detected 3 h after wounding (Table 1). This accumulation

declined at 8 h and then increased again at 24 and 48 h after the stress. However, the observed changes in *TaeMCAII* mRNA level during wounding were not statistically significant. A different expression pattern of *TaeMCAII* was observed after the heat-shock treatment. The transcripts level did not increase until 48 h after stress when they became elevated (Table 1). As revealed by ANOVA test the increase in *TaeMCAII* mRNA level during this stress is statistically significant at $P = 0.05$.

According to the *FFAS03* results, the best scoring template for the homology modelling of *TaeMCAII* was the crystal structure of the protein GSU0716 from *Geobacter sulfurreducens*, the *Northeast Structural Genomics* target *GsR13* (- 50.5 with 22 % of sequence identity) (3BIJ). The function of this experimentally resolved protein is not yet known, but the preliminary *BLAST* results show the presence of peptidase C14, caspase domain (pfam00656) and significant similarities to bacterial caspases (peptidases C14) with expect values in the range of 1e-80: 1e-16 and putative higher plants metacaspases from *Oryza sativa*, *Sorghum bicolor* and *Vitis vinifera* (*BLAST* e-values below 1e-09).

Strikingly, the surroundings of the key catalytic residues His and Cys (YSGHG and SDSCH) were

identical in GSU0716 and the *T. aestivum* metacaspase sequence (Fig. 4). As the second candidate for homology modelling template, the crystal structure of the human CASP7 in complex with the acetyl-Asp-Glu-Val-Asp-CHO reversible peptide inhibitor, was considered. The structure of CASP7 was already successfully used as a template for the modelling of the supposed AtMC9 (*A. thaliana* type II metacaspase) fold by Belenghi *et al.* (2007). Finally, the bacterial template has been selected for further analysis, because of the higher sequence similarity and significantly better *FFAS03* score. Global model accuracy (after validation by *MetaMQAP*) was: 37.371 GDT-TS (global distance test-total score) and 4.891 RMSD (root mean square deviation).

According to phylogenetic analyses (results of ML clustering are presented in Fig. 5), *TaeMCAII* clusters with type II plant metacaspases: *A. thaliana* metacaspase 9 (AtMC9), *Zea mays* type II metacaspase (ZmMCII), *Picea abies* metacaspase (mcII-Pa) and *Pinus silvestris* meta-caspase (PsMCII). The separate branch is created for *A. thaliana* type II metacaspases (AtMC1, AtMC2 and AtMC3) and *Ricinus communis* putative metacaspase sequence.

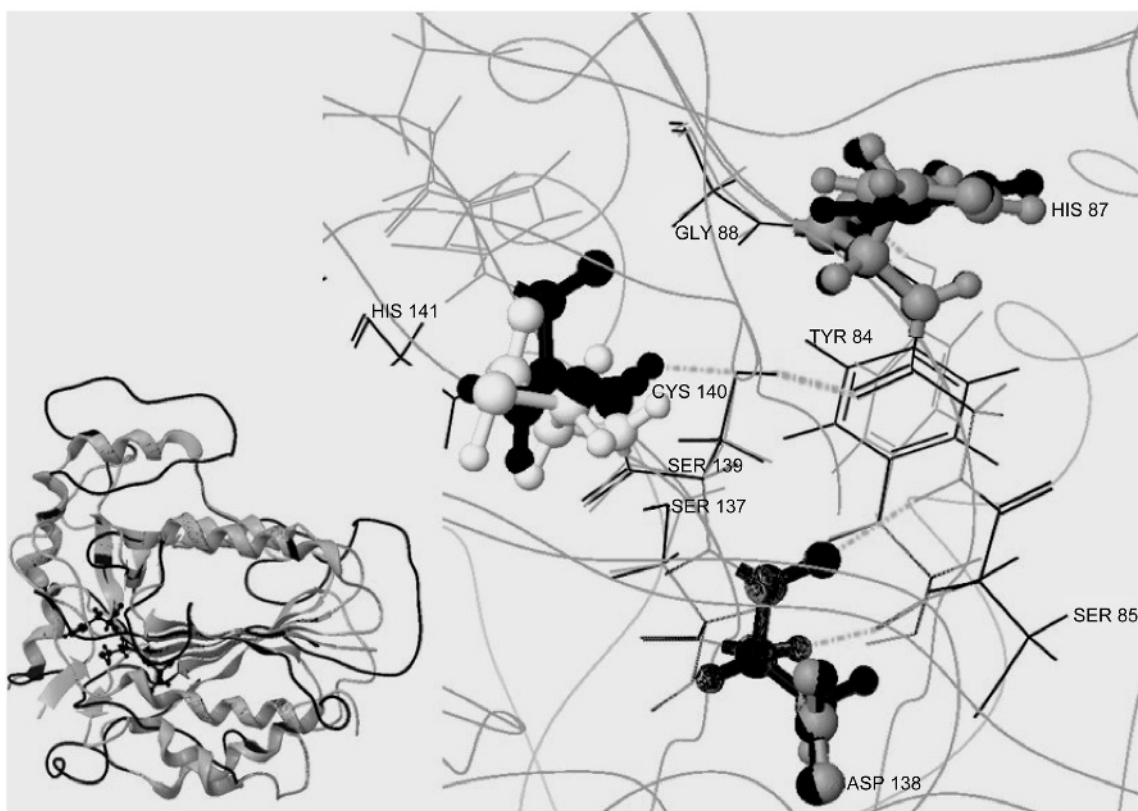


Fig. 4. Structural model of 3D fold of *TaeMCAII* obtained using homology modelling approach based on the crystal structure of protein GSU0716 from *Geobacter sulfurreducens* (3bij.pdb) as a template. Two conserved regions YSGHG and SDSCH are identical with corresponding motifs from *TaeMCAII* and other plant type II metacaspases. They both contain His and Cys catalytic residues that are depicted in ball and stick representation (black) (on the left). Positions of key residues from the modeled structure (ball and stick representation - white and grey): His 87 (white) Cys 140 (grey) and Asp 138 (dark grey) (on the right).

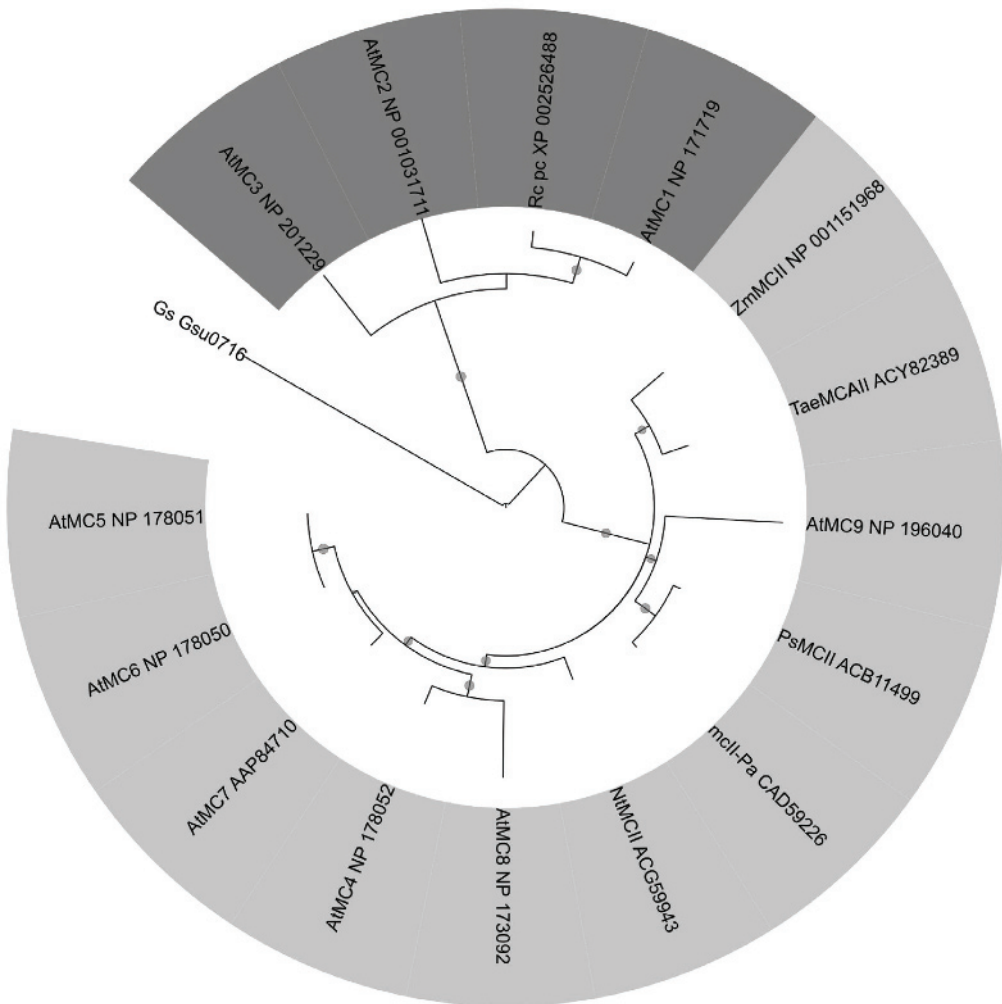


Fig. 5. Maximum likelihood tree for plant type I and type II metacaspases found in the second *PSI-BLAST* iteration. Clustering based on the MSA of 16 sequences. Color ranges: light grey: type II metacaspases from: *T. aestivum* (TaeMCAII-ACY82389), *Z. mays* (ZmMCII-NP_001151968), *P. abies* (mcII-Pa-CAD59226), *P. silvestris* (PSMCII-ACB11499), *N. tabacum* (NtMCII-ACG59943) and *A. thaliana*: (AtMC5-NP_178051, AtMC4-NP_178052, AtMC7-AAP84710, AtMC8-NP_173092, AtMC9-NP_196040), dark grey: type I metacaspases from *A. thaliana* (AtMC1-NP_171719, AtMC2-NP_001031711, AtMC3-NP_201229) and *R. communis*, Rc_pc (XP_002526488), Bacterial putative peptidase C14(caspase) sequence Gsu0716 (NP_951773.1) used as an outgroup for tree rooting. Circles depict approximate likelihood-ratio test (aLRT-SH-like) values greater than 75 %.

Discussion

The full-length sequence of the *TaeMCAII* cDNA was obtained from leaves of *T. aestivum* subjected to wounding stress. Because of its sequence, domain structure and lack of the characteristic N-terminal prodomain it can be classified as a type II metacaspase (Fig. 1; Uren *et al.* 2000, Vercammen *et al.* 2004). The successful sequencing of the whole genome of *Oryza sativa* allowed the identification of all genes encoding type I and type II metacaspases of rice, but the general characteristics of metacaspases cDNAs in cereals is still missing. Thus, this is the first report concerning the amplification and description of a full-length metacaspase

cDNA from cereal plants. A deduced protein encoded by the obtained metacaspase cDNA was 405 amino acids long with its catalytic centre in the large subunit and a conserved catalytic triad, His/Gly/Cys, similar to other plant metacaspases (Vercammen *et al.* 2004). As revealed by the MSA analysis, the replacement of an acidic residue, Asp, by Ser is present in the small subunit of TaeMCAII (Fig. 2). The influence of the mentioned substitution needs further investigation on the substrate specificity of TaeMCAII. Plant metacaspases identified so far cleave protein substrates after an Arg residue preferentially and to a lesser extent after a Lys residue

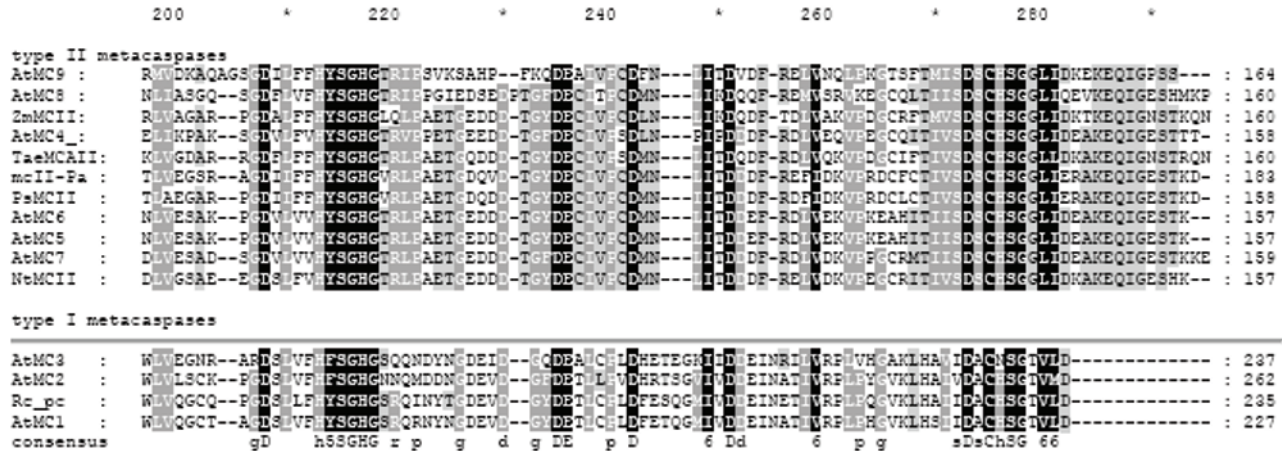


Fig. 6. Comparison of the large subunit catalytic domain sequences of plant type I and type II metacaspases. Surroundings of catalytic residues His87 and Gly88 are conserved in both groups of metacaspases, while the residues in the neighborhood of Cys140 differ between type I and type II metacaspases groups.

(Vercammen *et al.* 2006).

The metacaspase role in plant PCD or in plant cells proliferation and differentiation is still poorly understood. In this work, the attempt was made to investigate the role of a newly amplified type II metacaspase from wheat in PCD triggered by heat shock or wounding by measuring its transcript levels. Cells exposed to these abiotic stresses exhibited ultrastructural changes indicative of PCD, as revealed by the TEM analysis (Fig. 2). Leaf blade mesophyll cells displayed a similar timing and ultrastructural abnormalities of organelles common for either wounding or heat shock induced PCD. Typical features of both responses were the rupture of tonoplasts, the granulation and condensation of nuclear chromatin and the aberrant ultrastructure and the final destruction of chloroplasts observed as early as 3 h post-stress. The first mesophyll cells being empty and devoid of protoplast or containing remnants of protoplast were observed 8 h post stress. The PCD of individual cells was apparently not temporally coordinated, and it seems to be induced by an internal cell trigger because frequently dead and empty cells were found next to cells revealing the first PCD symptoms. Also minor changes like the deposition of electron-translucent material at the cell walls were similar in both responses. The main differences between both reactions concerns the protoplast clumping and rupture of the cell wall, allowing the leakage of the protoplast remnants into the intercellular spaces, which occurred in heat-induced PCD but not in wounding-induced PCD. It seems that both differences might be caused by the different nature of the implemented stress. In the case of heat-treated plants, the deposition of electron-translucent cell wall material was quite abundant at the plasmodesmata, and possibly the plasmodesmata were occluded and destroyed. Thus, the protoplasts lost their anchors, fixing them to the cell walls, and protoplasts

collapsed into large clumps. Also, cell-wall ruptures might be caused by the heat, which destroyed or blocked the machinery that controls the cell wall-degrading enzymes. Their uncontrolled action could weaken the cell walls and made them more fragile and susceptible to local destruction.

Though the increased levels of *TaeMCAII* mRNA were found at all of the time points after wounding stress except 8 h the observed changes did not occur to be statistically significant (Table 1). Maybe that wounding-induced PCD in wheat is a metacaspase-independent pathway or other wheat metacaspases may take part in proteolytic cascade during this process. Another *Arabidopsis* metacaspase gene *AtMCP1b* was found to be up-regulated during PCD triggered by wounding what supports the view that some metacaspases participate in PCD evoked by wounding (Castillo-Olamendi *et al.* 2007). The changes in *TaeMCAII* mRNA level during PCD induced by the heat-shock treatment, suggest that *TaeMCAII* may take part in the late stages of PCD induced by the heat-shock treatment, or that PCD triggered by heat shock may follow at least partly a metacaspase-independent pathway. Maybe the low level of *TaeMCAII* mRNA in this stress is caused by the low number of mesophyll cells that exhibit the hallmarks of PCD until 24 h after the stress. Moreover, there is a possibility that *TaeMCAII* is regulated on translational or post-translational levels under this stress conditions. Only a few investigations were conducted to elucidate metacaspases role in PCD triggered by abiotic stresses (Hoeberichts *et al.* 2003, Castillo-Olamendi *et al.* 2007, He *et al.* 2008). Many data concerning the metacaspase role and PCD seem contradictory. The metacaspase gene *LeMCA1* from *Lycopersicon esculentum* was not found to be up-regulated during PCD connected with an exposure to chemicals such as camptothecin and fumonisin B1, but

its transcription was increased in response to pathogen *Botrytis cinerea* infection (Hoeberichts *et al.* 2003). In contrast, staurosporine induced PCD, and the wounding of *A. thaliana* leaves led to the increased *AtMCP1b* mRNA levels (Castillo-Olamendi *et al.* 2007). Interestingly, only one, *AtMC8*, out of nine metacaspase transcripts studied in *A. thaliana* was found to be elevated during the PCD pathways induced by UV-C, H₂O₂ and methyl viologen (He *et al.* 2008). These data suggest that some metacaspases may play a role in PCD, and some may be involved in other processes. Metacaspase-independent PCD pathways may exist in plants. Furthermore, the investigations on the metacaspase activity regulation process would provide an exact explanation to these contradictory results.

It is known that all metacaspases are synthesised as inactive zymogens, and their activation is caused by autoproteolytic cleavage (Vercammen *et al.* 2004, Bozhkov *et al.* 2005). Autocatalytic cleavage sites were identified in the mcII-Pa sequence after residues Arg 188 in the large subunit and Lys 269 in the linker region (Bozhkov *et al.* 2005). According to Vercammen *et al.* (2004), in *A. thaliana* the metacaspase AtMC9 autocatalytic site is placed after the Arg 214 residue. Based on the MSA analysis, we can confirm the conservation of the Lys 260 and Arg 214 residues, the counterparts of Lys 269 and Arg 214 from mcII-Pa and AtMC9, respectively. In the surroundings of TaeMCAII active site Cys 140 there is the motif DSCHSG which is highly conserved among all type II plant metacaspases (Fig. 6). In type I metacaspases there are two substitutions within this motif: residue Ser 139 (numbering according to TaeMCAII sequence) is replaced by Ala and instead of His 141 Asn may occur.

References

Baarlen, P., Woltering, E.J., Staats, M., Van Kan, J.A.L.: Histochemical and genetic analysis of host and non-host interactions of *Arabidopsis* with three *Botrytis* species: an important role for cell death control. - Mol. Plant. Pathol. **8**: 41-54, 2007.

Belenghi, B., Romero-Puertas, M.C., Vercammen, D., Brackenier, A., Inze, D., Delledonne, M., Van Breusegem, F.: Metacaspase activity of *Arabidopsis thaliana* is regulated by S-nitrosylation of a critical cysteine residue. - J. biol. Chem. **282**: 1352-1358, 2007.

Bonneau, L., Ge, Y., Drury, G.E., Gallois, P.: What happened to plant caspases? - J. exp. Bot. **59**: 491-499, 2008.

Bozhkov, P.V., Suarez, M.F., Filonova, L.H., Daniel, G., Zamyatnin, A.A., Rodriguez-Nieto, S., Zhivotovsky, B., Smertenko, A.: Cysteine protease mcII-Pa executes programmed cell death during plant embryogenesis. - Plant. Biol. **102**: 14463-14468, 2005.

Castillo-Olamendi, L., Bravo-Garcia, A., Moran, J., Rocha-Sosa, M., Porta, H.: AtMCP1b, a chloroplast-localised metacaspase, is induced in vascular tissue after wounding or pathogen infection. - Func. Plant Biol. **34**: 1061-1071, 2007.

Chomczyński, P., Sacchi, N.: Single-step method of total RNA isolation by a single extraction with an acid guanidinium thiocyanate-phenol-chloroform extraction. - Anal. Biochem. **162**: 156-159, 1987.

Golinowski, W., Grundler, F.M.W., Sobczak, M.: Changes in the structure of *Arabidopsis thaliana* during female development of the plant-parasitic nematode *Heterodera schachtii*. - Protoplasma **194**: 103-116, 1996.

Hao, L., Goodwin, P.H., Hsiang, T.: Expression of a metacaspase gene of *Nicotiana bentamiana* after inoculation with *Colletotrichum destructivum* or *Pseudomonas syringae* pv. *tomato*, and the effect of silencing the gene on the host response. - Plant. Cell Rep. **26**: 1879-1888, 2007.

He, R., Drury, G.E., Rotari, V.I., Gordon, A., Willer, M., Farzaneh, T., Woltering, E.J., Gallois, P.: Metacaspase-8 modulates programmed cell death induced by UV and H₂O₂ in *Arabidopsis*. - J. biol. Chem. **283**: 774-783, 2008.

Hoeberichts, F.A., Have, A., Woltering, E.: A tomato metacaspase gene is upregulated during programmed cell death in *Botrytis cinerea*-infected leaves. - Planta **217**: 517-522, 2003.

The replacement of polar Ser by aliphatic Ala can influence substrate specificity of those two families of plant metacaspases.

A prediction of the three-dimensional protein structure of TaeMCAII with the known crystal structure of the bacterial protein GSU0716, as a template, seems to confirm the tertiary structural homology of metacaspases with their bacterial homologs (Fig. 4). According to obtained model conserved motifs including catalytic residues Cys 140 (SDSCH) and His 87 (YSGHG) create parallel loops which form a kind of binding grove and are connected by several H-bonds. Unfortunately, there is no available structure for any complex of GSU0716 and the ligand in the PDB database; hence there is no possibility to investigate the active site residues relation and contacts with the potential ligand. The relative positions of Cys 140, His 87 and Asp 138, which makes a distinct feature between caspase type active site and its metacaspase counterpart, denote a kind of catalytic triangle. Asp 138 makes H-bonds with two residues from parallel motif YSGHG: Tyr 84 and Ser 85, what can confirm the significance of these two residues conserved among all analyzed plant metacaspases. Ser 137 which differentiates type II from type I metacaspases is located between Cys 140 and Asp 138 because of the loop turn and may be important for substrate specificity of these two groups of enzymes.

Phylogenetic analyses revealed that TaeMCAII is the closest relative of *Z. mays* type II metacaspase and has a common ancestor with all *A. thaliana* type II metacaspases and with so far identified type II metacaspases from another higher plants *P. silvestris*, *P. abies* and *N. tabacum* (Fig. 5).

Jacobson, M.P., Pincus, D.L., Rapp, C.S., Day, T.J.F., Honig, B., Shaw, D.E., Friesner, R.A.: A hierarchical approach to all-atom loop prediction. - *Proteins* **55**: 351-367, 2004.

Letunic, I., Bork, P.: Interactive Tree Of Life (iTOL): An online tool for phylogenetic tree display and annotation. - *Bioinformatics* **23**: 127-128, 2007.

Liu, Y., Schiff, M., Czymbek, K., Talloczy, Z., Levine, B., Dinesh-Kumar, S.P.: Autophagy regulates programmed cell death during the plant innate immune response. - *Cell* **121**: 567-577, 2005.

Pawlowski, M., Gajda, M.J., Maślak, R., Bujnicki, J.M.: MetaMQAP: a meta-server for the quality assessment of protein models. - *BMC Bioinformatics* **29**: 9-403, 2008.

Rychlewski, L., Jaroszewski, L., Li, W., Godzik, A.: Comparison of sequence profiles. Strategies for structural predictions using sequence information. - *Protein Sci.* **9**: 232-241, 2000.

Sobczak, M., Grundler, F.M.W., Golinowski, W.: Changes in the structure of *Arabidopsis thaliana* roots induced during development of males of the plant parasitic nematode *Heterodera schachtii*. - *Eur. J. Plant. Pathol.* **103**: 113-124, 1997.

Uren, A.G., O'Rourke, K., Aravind, L., Pisabarro, M.T., Seshagiri, S., Koonin, E.V., Dixit, V.M.: Identification of paracaspases and metacaspases: two ancient families of caspase-like proteins, one of which plays a key role in MALT lymphoma. - *Mol. Cell* **6**: 961-967, 2000.

Vercammen, D., Belenghi, B., Van de Cotte, B., Beunens, T., Gavigan, J.A., De Rycke, R., Brackenier, A., Inze, D., Harris, J.L., Van Breusegem, F.: Serpin 1 of *Arabidopsis thaliana* is a suicide inhibitor for metacaspase 9. - *J. mol. Biol.* **364**: 625-636, 2006.

Vercammen, D., Van de Cotte, B., De Jaeger, G., Eeckhout, D., Casteels, P., Vanepoel, K., Vandenbergh, I., Van Beeumen, J., Inze, D., Van Breusegem, F.: Type II metacaspases Atmc4 and Atmc9 of *Arabidopsis thaliana* cleave substrates after arginine and lysine. - *J. biol. Chem.* **279**: 45329-45336, 2004.

Watanabe, N., Lam, E.: Recent advance in the study of caspase-like proteases and Bax inhibitor-1 in plants: their possible roles as regulator of programmed cell death. - *Mol. Plant Pathol.* **5**: 65-70, 2004.

Zhu, K., Shirts, M.R., Friesner, R.A.: Improved methods for side chain and loop predictions via the protein local optimization program: variable dielectric model for implicitly improving the treatment of polarization effects. - *J. Chem. Theory Comput.* **3**: 2108-2119, 2007.